Nordic Hydrology, 28 (3), 1997, 169-188

Adaptive Use of a Conceptual Model for Real Time Flood Forecasting

D. Da Ros and M. Borga

Dept. of Land and Agroforest Environments,
University of Padova, Italy

This paper investigates the adaptive use of a simple conceptual lumped rainfall-runoff model based on a Probability Distributed Model complemented with a Geomorphological Unit Hydrograph. Three different approaches for updating the model and for its use for real time flood forecasting are compared: the first two are based on a parameter updating approach; in the third procedure the model is cast into a state-space form and an Extended Kalman Filter is applied for the on-line estimation of the state variables. The comparison shows that the procedure based on the filtering techniques provides more reliable results; acceptable results are also obtained by using a parameter updating approach based on the on-line adjustment of the initial conditions.

Introduction

The importance of timely flood warnings and improved flood management is increasingly recognised. In several countries damage due to floods shows a consistent upward trend, in relation to increasing population pressure on flood plains and to the development of river basins. In this context, flood forecasting and early warning becomes instrumental in saving lives and property. Rainfall-runoff models that are able to operate within an adaptive mode are often used to provide real time discharge forecasting (Wood and O'Connell 1985; Todini 1989). In particular the use of a conceptual model for real time forecasting purposes is generally achieved through the coupling of a rainfall-runoff simulation model and a procedure for forecasting updating (Serban and Askew 1991). Several possibilities for adaptive forecasting exist with conceptual models.

This paper investigates the adaptive use of a simple conceptual lumped rainfall-runoff model based on a Probability Distributed Model (PDM) (Moore and Clarke 1981; Moore 1985) complemented with a Unit Hydrograph (UH) derived on geomorphological basis (Gupta *et al.* 1986). Three different adaptive procedures are compared for a mid-size basin located in north-eastern Italy. The first two procedures are based on a parameter updating approach: the model parameters are adjusted so that the required agreement between forecasted and observed discharges in a least squares sense is obtained; the procedures differ from one another as to the number of parameters involved in the on-line calibration. In the third procedure the model is cast into state-space form and an Extended Kalman Filter (EKF) is applied for the on-line estimation of the state variables.

Experimental Basin and Hydrometeorological Data

The study region is the Bacchiglione river basin closed at Montegaldella (Fig. 1); it has a drainage area of 1,384 km^2 and is located in north-eastern Italy. Elevation ranges between 15 m a.s.l. at the basin outlet and 2,341 m a.s.l., with an average value of 649 m a.s.l.. Mean annual precipitation ranges from 1,050 to 2,200 mm over the basin. Eight major flood events, which occurred in the period 1941-1978, were selected for this study. Hourly precipitation data were collected from a raingauge network of ten tipping-bucket instruments, whose locations are displayed in Fig. 1. Mean areal precipitations were computed by using Thiessen polygons. Table 1 reports a brief description of each event in terms of peak discharge, maximum rainrate and mean areal cumulative rainfall. Three events were treated as calibration events (storms 1 to 3), and the remaining ones (storms 4 to 8) were retained for validation purposes.

We recognize that a lumped approach, as the one followed in this study, could be questioned for a basin of this size; for instance, the UK Flood Studies Report (NERC 1975) recommends that such approach should not be used on catchments with an area larger than 500 km^2, where the assumption of nearly uniform net rainfall over the catchment cannot be justified. However, operational experience and past research show that paucity of rainfall information from raingauges in real time imposes a limit on model performance and force to follow a lumped approach even for large basins (Georgakakos and Smith 1990; WMO 1992). Detailed information on rainfall space-time structure, obtained from weather radar and a dense raingauge network, is available for the study area only in recent years (Bacchi and Borga 1993; Bacchi *et al.* 1996; Borga and Vizzaccaro 1996). Results from a study on the influence of rainfall spatial variability on accuracy of real-time flood forecasting are reported in a forthcoming paper.

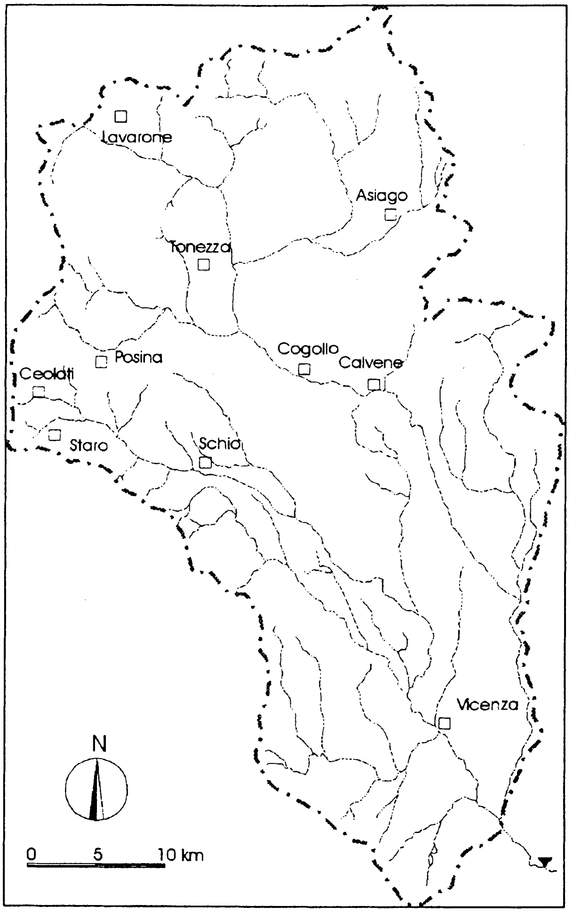

Fig. 1. The Bacchiglione river basin closed at Montegaldella (1,384 km^2) and the location of the raingauges.

Table 1 – Characteristics of flood events

No	Date of flood peak	Max rainrate [mm/h]	Mean and total rainfall [mm]	Peak discharge [m^3/s]
1	14.11.1941	13.9	224.1	362
2	01.06.1965	7.7	64.3	243
3	15.01.1969	8.2	111.4	330
4	28.09.1965	12.1	185.3	282
5	17.11.1968	10.6	164.7	363
6	18.11.1975	10.7	102.7	277
7	14.05.1977	15.3	165.5	267
8	26.02.1978	6.7	86.7	261

Description and Application of the Model

In the hydrological model used for this research, the runoff formation process is modelled through the PDM, while a linear transfer function derived on geomorphological basis is used to simulate the runoff routing process. A description of these submodels is provided here.

Following the probability-distributed principle, in the PDM only the frequency of hydrological variables of certain magnitudes over the basin is considered, without regard to the localisation of a particular occurrence within the basin; this is done by representing the process of interception and soil moisture storage by means of a statistical population of stores instead of a single storage component. Then, the selection of a probability distribution describing the spatial variation of process parameters over the basin is used to derive algebraic expressions for the integrated response from the basin. The basin is considered to be made of a population of stores, each one characterised by its store capacity c, and water is allowed to redistribute among stores in such a way as to cause all storage elements have an equal depth of water, C^*, except those with depth less than C^* which are full. The depth of water in a storage is increased by rainfall P, and generation of runoff occurs when rainfall exceeds the storage capacity c. The depth c is viewed as a random variate with probability density function (*pdf*) $f(c)$ and cumulate distribution function $F(c)$; the Rayleigh function (Moore and Clarke 1981), specified by the parameter σ (see Appendix A), is adopted as the *pdf* for the depth c. This function was chosen because it is parsimonious as the number of parameters involved and it is continuous and not bounded.

The instantaneous rate of runoff generation from the basin, $q(t)$, is obtained by multiplying the rainfall rate by the proportion of the basin which is saturated. In this way, the volume of direct runoff generated in the time interval $[t\text{-}\Delta t, t]$ is

$$V(t) = \int_{t-\Delta t}^{t} q(\tau)\,d\tau = \int_{C^*(t-\Delta t)}^{C^*(t)} F(c)\,dc \qquad (1)$$

where

$$C^*(t) = C^*(t-\Delta t) + P_t \Delta t \qquad (2)$$

where P_t is the rainrate in the time interval $[t\text{-}\Delta t, t]$. The difference between precipitation and runoff volumes represents the addition to soil moisture storage.

Direct runoff generated from the spilling of a full storage element is routed to the basin outlet by means of a transfer function independently of runoff from neighbouring elements. Since data are available at discrete time intervals (in the following application the time interval Δt is taken equal to 1 hour) it is easier to use a discrete convolution integral; hence, the discharge at the outlet of the basin is obtained as follows

$$Q_{i\Delta t} = Q(i\Delta t) = A \int_0^{i\Delta t} q(\tau) u(i\Delta t-\tau)\, d\tau = A\, \underline{u}^T \underline{V}(i) \tag{3}$$

where A represents the basin area, $u(t)$ is the transfer function (Instantaneous Unit Hydrograph, IUH), u is the n-vector of the Unit Hydrograph (UH), obtained from the integration of the IUH function, $n\Delta t$ represents the UH time base, and $V(i)$ is the n-vector

$$\underline{V}^T(i) = \left[\int_{C^*_{i-1}}^{C^*_i} F(c)\, dc \quad \int_{C^*_{i-2}}^{C^*_{i-1}} F(c)\, dc \quad \ldots \quad \int_{C^*_{i-n}}^{C^*_{i-n+1}} F(c)\, dc \right]^T \tag{4}$$

The last term of Eq. (3) is particularly suitable for the application of the updating schemes that will be presented in the next section. Following Eq. (3), the discharge per unit area at the outlet of the basin can be seen as the scalar product of the time-invariant vector u with the vector $V(i)$.

A geomorphological approach is followed for the derivation of the IUH. Motivation for such choice is essentially that river network routing models which rely on topographic variables, such as the Geomorphological Unit Hydrograph, allow to incorporate, in a compact way, digitised river network data. In this study, the basin response function is broken down into a hillslope response function and a network response function. The basin IUH $u(t)$ is assumed to result from the convolution of the network response function $u_n(t)$ and the hillslope response function. This subdivision seems to be particularly appropriate for large basins in which the network response may dominate the overall basin response (Naden 1992). As to the channel network, its IUH is seen as the holding time probability distribution function of a drop of water once it enters the channel network. This *pdf* is computed by using the network geometry and a single routing function governing water transport from any point in the network to the outlet (Gupta *et. al.* 1986; Mesa and Mifflin 1986). The same response function $g(t,x)$ is assumed for all points at equal distance x from the outlet, which means that the different geometric and hydrodynamic characteristics of each pathway characterised by distance x cannot be distinguished from one another at the basin scale. The response of the network as a whole is derived on the basis of the averaged flow equation $g(t,x)$ and of the width function $N(x)$, which represents the frequency distribution of channels with respect to flow distance x from the outlet (Kirkby 1976; Mesa and Mifflin 1986). In this study the width function was derived from digitised river network data based on the 1:50.000 IGM maps of Italy.

Thus if a unit volume of runoff is generated instantaneously and uniformly over the river network, the probability that this volume will be injected at a flow distance comprised in the interval $[x, x + dx]$ is expressed by the product $Z^{1}N(x)dx$ where Z denotes the total network length; the Geomorphological Instantaneous Unit Hydrograph (GIUH) is then computed by summing the partial transfer function over the network weighted by these probability values

$$u_n(t) = \int_0^\infty Z^{-1} N(x) g(t,x) dx \tag{5}$$

In order to account for attenuation of the flood peak due to channel and flood plain storage, which are important in large basins, the inverse Gaussian Green's function (Gupta *et al.* 1986) was used in this study as flow equation $g(t,x)$. This function is the solution of the linear advection-dispersion equation, which represents the diffusion-analogy simplification of the linearised version of the St. Venant equations. Because of the discrete nature of the network width function, Eq. (5) was integrated over incremental distances in the following way

$$\tilde{u}_n(t) \cong \sum_{i=1}^{n} \frac{x_i}{(4\pi D t^3)^{1/2}} \exp\left(-\frac{(x_i - vt)^2}{4Dt}\right) \frac{N(x_i)}{Z} (x_i - x_{i-1}) \tag{6}$$

where x_i denotes the distance of the node i from the outlet, v is the wave celerity, while the dispersion term D reflects the tendency of the wave to disperse while propagating, as a result of the turbulence and shearing effects. A triangular shape was used to represent the hillslope response, and its base time was determined on the basis of physical considerations and with reference to previous studies on the basin (Chander and Fattorelli 1989; Borga *et al.* 1991), in order to obtain a lag time for the whole transfer function consistent with findings by these authors.

In this study, model applications concern only the direct component of the hydrograph. Results obtained in this way can be considered representative of operational real time forecasting systems based on event-type models, where forecasted discharges are generally added to the discharge observed at the starting time of the event.

As a first step, the model was calibrated on the basis of the storms 1 to 3. A unique set of parameters D and v was identified, while a different couple σ and C^*_0 was estimated for each event. The base time of the UH is equal to 28 hours. Table 2 reports the estimated parameter values together with an assessment of the calibration in terms of the root mean square error (RMSE), while Fig. 2 reports an example of the calibration results. A wide interstorm variability is apparent for both σ and C^*_0. It

Table 2 – Off-line calibration results

Event	Estimated σ [mm]	Estimated C^*_0 [mm]	RMSE [$m^3 s^{-1}$]
14.11.1941	362	83	15.4
01.06.1965	136	46	12.8
15.01.1969	306	71	7.5

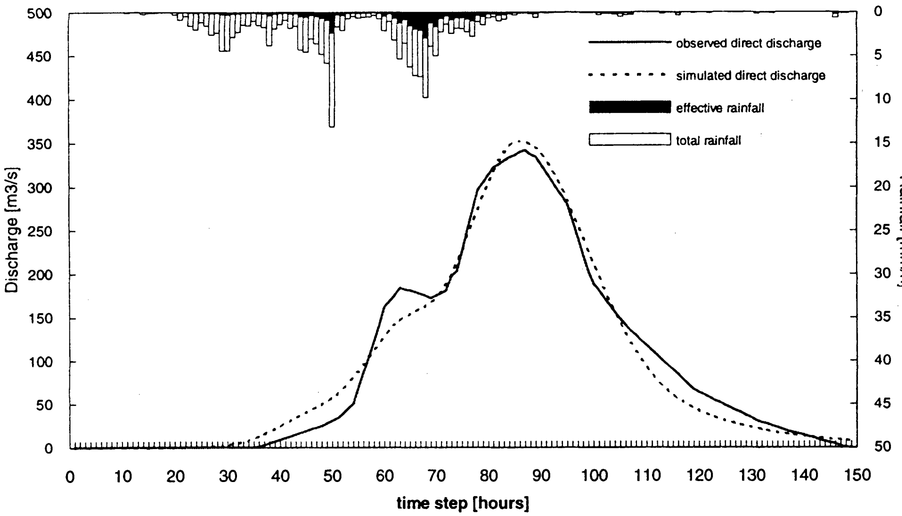

Fig. 2. Observed and simulated direct discharge after the off-line automatic calibration for the November 1941 event (estimated values: σ = 362 mm, C^*_0 = 83 mm).

should be noted that this variability can be expected for C^*_0, which depends on the basin saturation condition at the beginning of the event, while this is not true for σ, which is related to the maximum storage capacity at the basin scale, and then should be a constant or vary with the season. It is speculated that the variability which affects σ represents the results of data errors and model inadequacy in representing the real processes.

Concerning the application of on-line updating techniques, in the forecasting stage actual precipitation data were used as input data, instead of forecasted values of input variables as the case would be in true real time operation. This 'perfect foresight' scenario was used in an effort to examine the performance of the hydrologic model free from the dominating inconsistencies between model forecasts and observations of streamflow caused by forecast-input errors. In this respect the study presented here indicates upper bounds of performance rather than typical performance of the model under real time conditions.

Updating Procedures

To obtain optimal benefit of real time runoff measurements in the forecasts, some sort of updating of the hydrological model is usually required, before a forecast is made. A feedback control structure would therefore characterise the model in order to achieve such a requirement (O'Connell and Clarke 1981; Moore 1986; Serban and Askew 1991, among others). In this study, the analysis is focused on two updating techniques:

a) on-line parameter adjustment, where one or more of the model parameters are updated until the model predictions and measured flows are in close agreement;
b) on-line state adjustment, where generally corrections are made for the water content of internal storages to achieve closer correspondence between measured and predicted flow.

On-line Parameter Adjustment

Both in on-line and off-line cases, automatic calibration is performed by searching for appropriate values of the parameters within the hyperspace generated by all their possible combinations. This is accomplished through the following steps:

a) specification of a measure of closeness between the output of the model and observed discharges (estimation criterion);
b) selection of a method for identifying those parameter values that optimise the estimation criterion, that is maximise or minimise an objective function.

As to the first step, in this study the simple least squares (SLS) estimation is used; this is the most common choice, although it is often arbitrary in spite of its importance in parameter estimation. Nevertheless, even though the SLS estimation is not considered an optimal procedure (likewise the maximum likelihood criterion) because of the autocorrelation and the heteroschedasticity of the residuals (Sorooshian and Dracup 1980), Brath and Rosso (1993) showed that its application to on-line parameter estimation provides reliable results for real time flow forecasting problems, while being less time-consuming than more complex procedures.

Because of the structural complexity of most conceptual rainfall-runoff models, the optimisation algorithms most frequently used to identify the parameters belong to the class of 'direct-search' procedures, while gradient-based techniques are seldom used (Gupta and Sorooshian 1985). Thanks to the differentiability of the objective function, the parameter estimation is achieved in this study by using a gradient-based technique, that is the Gauss-Newton method. The formulation of the algorithm is detailed in Appendix A. The algorithm is applied in two different versions: in the first case two parameters are updated, and are the initial condition C^*_0 and parameter σ; in the second case the value of s is kept fixed and equal to 270 mm, on the basis of calibration on events 1 to 3, and only the initial condition is optimised online.

Filtering

A common method used for adaptive estimation in real time flow forecasting involves the use of Kalman filter (Bras and Rodriguez-Iturbe 1985; Wood and O'Connell 1985). This filter is essentially a data processing algorithm by which observed discharges are used to automatically update the model states (Kitanidis and Bras 1980a; Georgakakos 1986; Georgakakos and Smith 1990).

The use of the Kalman filter requires the model to be expressed in a state-space formulation, consisting of two equations:

the state equation

$$\underline{X}_t = \Phi \underline{X}_{t-1} + \underline{G} U_t + \underline{\Gamma} w_t \tag{7}$$

and the observation equation

$$z_t = h(\underline{X}_t) + v_t \tag{8}$$

where X_t represents the vector of state variables, consisting of the critical capacities that enter in the computation of the discharge at the time t, U_t – the input variable – is the rainfall aggregated in the interval (t- Δt, t), the matrix Φ is the state transition matrix, w_t and v_t are independent discrete dynamics and observations Gaussian white-noises with variances Q_t and R_t respectively. A more complete presentation of Eqs. (7) and (8) and definition of G and Γ are provided in Appendix B.

The discharge at the basin outlet is the observation variable. The observation Eq. (8) is constituted by the derivation of the direct runoff from the critical capacities values and its subsequent discrete convolution to the basin outlet, as described in Eq. (3) and can be expressed as

$$h(\underline{X}_t) = \underline{u}^T \underline{V}_t = \sum_{i=1}^{n} u_i V_i^t = \sum_{i=1}^{n} u_i \int_{C^*_{t-1}}^{C^*_{t-i+1}} F(c)\,dc = \sum_{i=1}^{n} u_i \int_{X^t_{i+1}}^{X^t_i} F(c)\,dc \tag{9}$$

It is well-known that in the case of linear dynamic systems, a Gaussian conditional distribution for the states results if the dynamic and observation noises are Gaussian, implying that the state's conditional expectation can be obtained through the Kalman filter. In the case of non linear dynamic systems, the conditional distribution for the states will be non Gaussian. This problem of state estimation is solved here by applying the Extended Kalman Filter. Aspects concerning the linearisation of the filter and the formulation of the Extended Kalman Filter are reported in Appendix B. Given measured outputs up to the including time t an estimate of X_t is computed, and the forecast of the future states and the corresponding discharges are accomplished in a deterministic way, according to updated soil storage contents.

In this case, the value of σ is kept fixed and equal to 270 mm, as in the preceding case, while the estimate of the initial soil storage content is computed for each flood event based on the discharge at the beginning of the event. An empirical, linear relationship between the initial soil storage content and the initial discharge was established based on analysis of flood events used for model calibration.

As to the noise statistics required by the model, the variance of the error of the state equation can be related to the uncertainties both in the conceptualisation of the runoff production process and in the mean areal precipitation estimation, while the noise term added to the observation equation is related to the measurement errors of the discharge. In the present case study an uncertainty was supposed to affect the discharge measures, even though the noise variance was assumed to be small; this choice prevents instabilities that can arise in the case the filter is forced to strictly follow the observed hydrograph. Furthermore, input and observation errors were modelled as stationary processes even though a model based on nonstationary random sequences, in which the errors increase with the magnitude of the observations, would be more realistic (Puente and Bras 1987; Georgakakos and Smith 1990).

Results and Comments

The forecast performances of the three methods were compared in terms of three statistical indexes. They are the root mean square error *RMSE*, the coefficient of efficiency C_E and the coefficient of persistence C_P (Kitanidis and Bras 1980b) and were computed for each event and for 4 different lead times: 2 hours, 4 hours, 6 hours and 8 hours. The coefficient of efficiency is a measure of the variance explained by the model and it takes the value of one for perfect performance. The coefficient of persistence compares the performance of the model with that of a naive model that predicts the current observation at each time step. Positive values of the coefficient are desirable; negative values indicate that the performance of the hydrologic model is worse (in a least-squares sense) than the performance of the naive model. Only the rising limb of the hydrograph and a short period beyond the peak time were considered in the computation. These statistics are reported in Table 3 and in Fig. 3. Analysis of these results reveals that the method based on the filtering of the state variables performs better in all cases except one, while the worst method is that based on the on-line estimation of both parameters. The procedure based on the on-line estimation of one parameter performs nearly as well as that based on the Extended Kalman Filter.

Table 3 – Coefficient of persistence (C_p) obtained by applying the three updating techniques for four lead times ranging from 2 to 8 hours

	2 h ahead for.			4 h ahead for.			6 h ahead for.			8 h ahead for.		
	LSE σ, C^*_0	LSE C^*_0	EKF	LSE σ, C^*_0	LSE C^*_0	EKF	LSE σ, C^*_0	LSE C^*_0	EKF	LSE σ, C^*_0	LSE C^*_0	EKF
Feb. 78	-8.25	-1.35	0.47	-3.39	0.13	0.60	-2.71	0.43	0.65	-2.77	0.55	0.69
May 77	-0.16	0.46	0.84	0.25	0.76	0.90	0.29	0.81	0.93	0.25	0.81	0.94
Sep. 65	-11.20	-3.70	0.20	-3.17	0.47	0.56	-1.66	0.17	0.66	-1.14	0.40	0.71
Nov. 68	-0.25	0.12	-0.47	0.41	0.70	-0.38	0.50	0.83	-0.34	0.47	0.87	-0.28
Nov. 75	-28.96	-1.25	0,50	-9.38	0.13	0.63	-5.43	0.43	0.65	-3.83	0.54	0.65

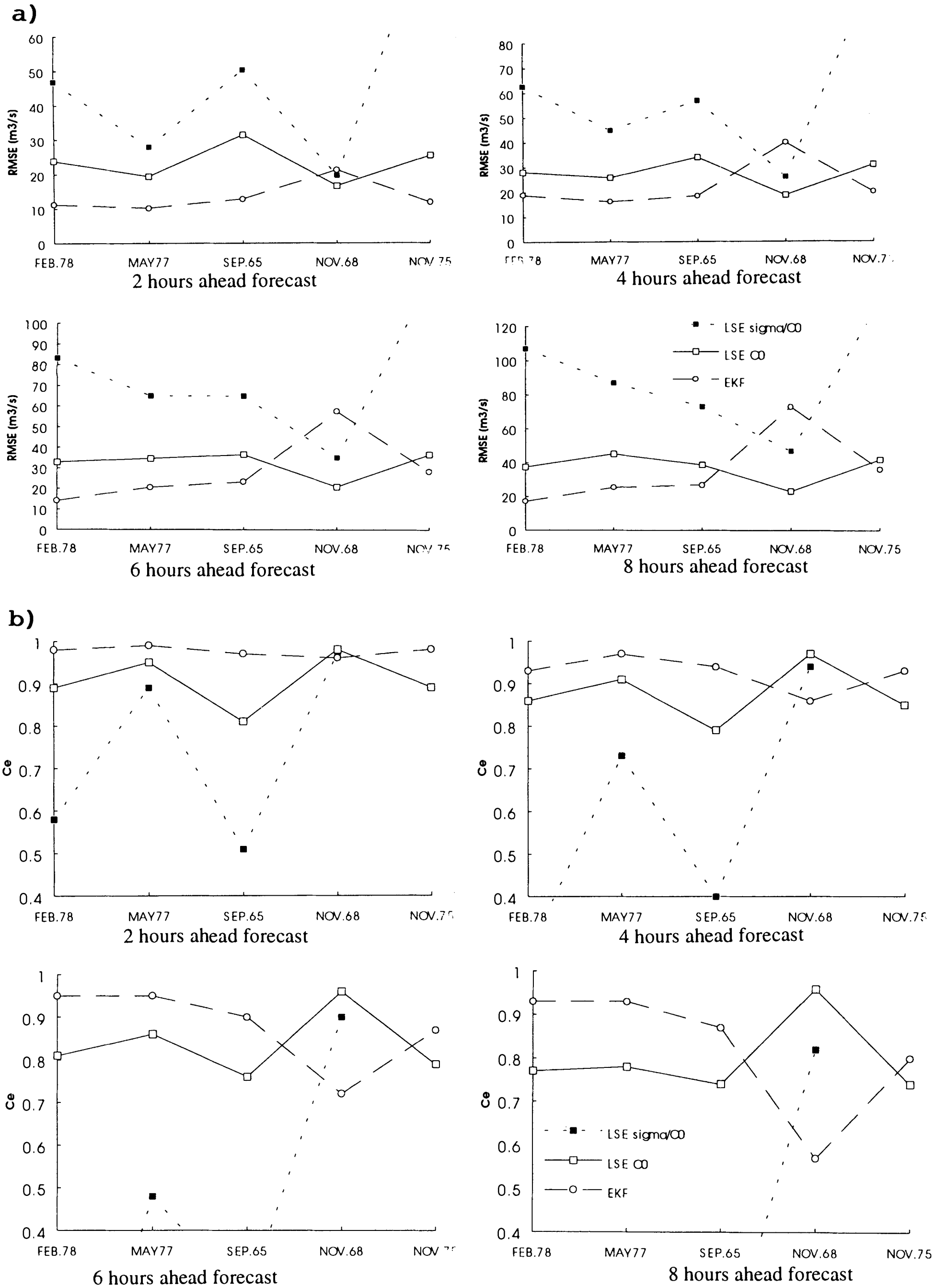

Fig. 3. Comparison of the performances in forecast for the three methods in terms of root mean square errors (RMSE) and coefficient of efficiency (C_e).

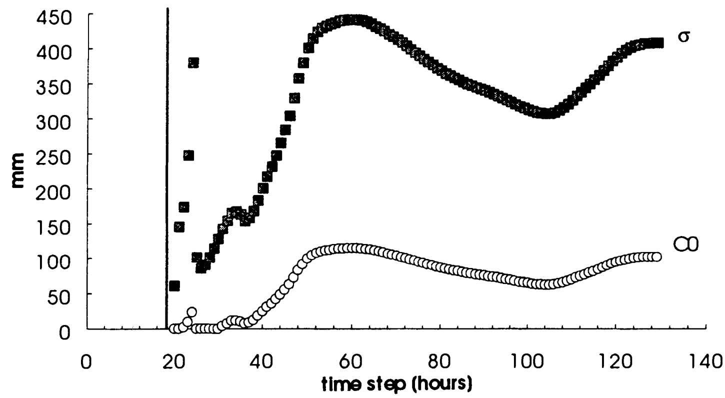

Fig. 4. Fluctuations of estimated values of σ and C^*_0 in the course of the adaptive calibration procedure for the May 1977 event.

It is suggested that the forecasting failure of the procedure based on the on-line estimation of both parameters occurs because the values of the parameters estimated at the 'now' are not representative of the behaviour of the basin for the forecasting lead time. Adaptive calibration would necessarily involve fluctuations of parameter estimates as these are progressively computed in the course of a flood event. However, if these fluctuations are too wide and rapid they can lead to model instability in the forecasting stage. Fig. 4 illustrates the fluctuations of the estimated values of parameters (σ_n, C^*_{0n}) in the course of the adaptive calibration procedure for the May 1977 event; the subsequent forecast is shown in Fig. 5. From the analysis of these latest figures two observations arise:

a) the parameters tend to fluctuate quite accordingly to each other until a stable configuration is achieved;
b) the erratic behaviour of both parameters results in a poor forecast ability of the model, especially for large lead times.

The first aspect is related to the shape of the objective function in the course of the event. In fact, it can be shown that, for each time step, the two-dimensional representation of the objective function has an elliptic configuration, with an orientation of the major axes along the bisecting line of the co-ordinated axes, slightly varying during the event. The optimum parameter set is found along such direction. Due to this reason the adaptive calibration in the course of the event implies that an increment in the value of one parameter corresponds to an increment of the other parameter, and *vice versa*.

As shown in Table 3 and Fig. 3, better results were obtained by keeping the value of s fixed and applying a monodimensional optimising algorithm for the on-line estimation of the initial condition C^*_0. Though the variability of C^*_{0n} is significant also in this case, the predictive ability of the model increases and a more stable be-

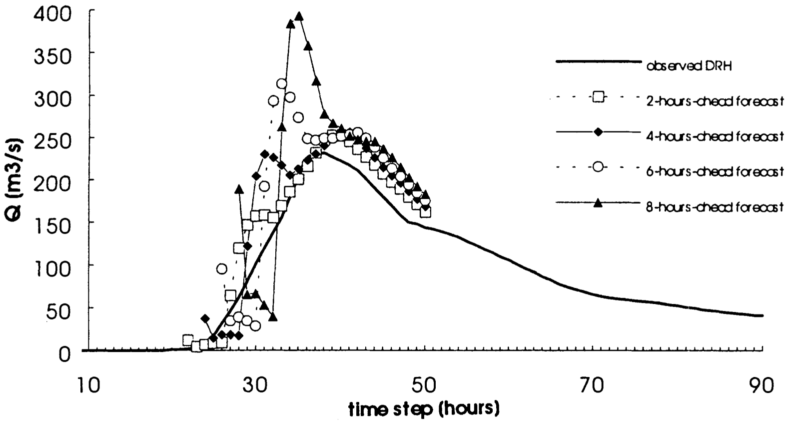

Fig. 5. Observed direct runoff hydrograph and 2-4-6-8 hours ahead forecasts by means of the on-line optimization of parameters σ and C^*_0 for the May 1977 event.

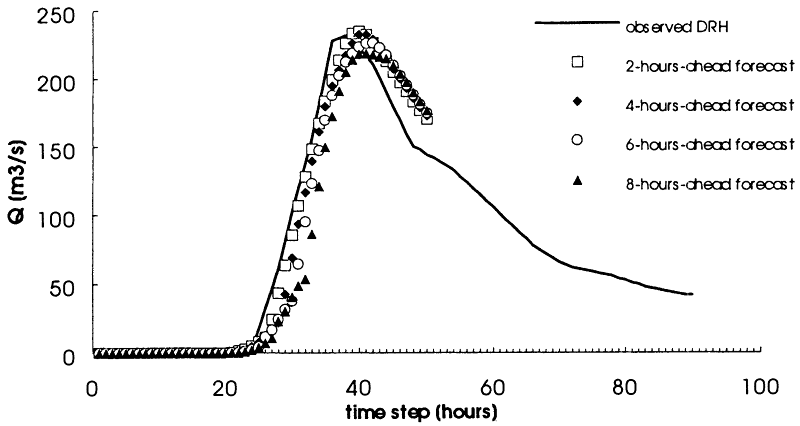

Fig. 6. Observed direct runoff hydrograph and 2-4-6-8 hours ahead forecasts by means of the on-line optimization of the initial condition C^*_0 for the May 1977 event (the value of σ was assumed to be 270 mm).

haviour is achieved. However, as shown in Fig. 6, this procedure leads to a poor forecasting performance in the first hours of the events, namely it results in the inability of the model in predicting in a correct way the beginning of the rising limb of the hydrograph.

The application of the Kalman filter algorithm for the on-line updating of soil moisture contents (Fig. 7) resulted both in a good simulation up to the time of the forecast with an improvement respect to the simulation-mode response of the model and in a better forecasting ability. In particular the model behaves in a more stable way when its results are compared with those of the other procedures, with an increased reliability of the prediction.

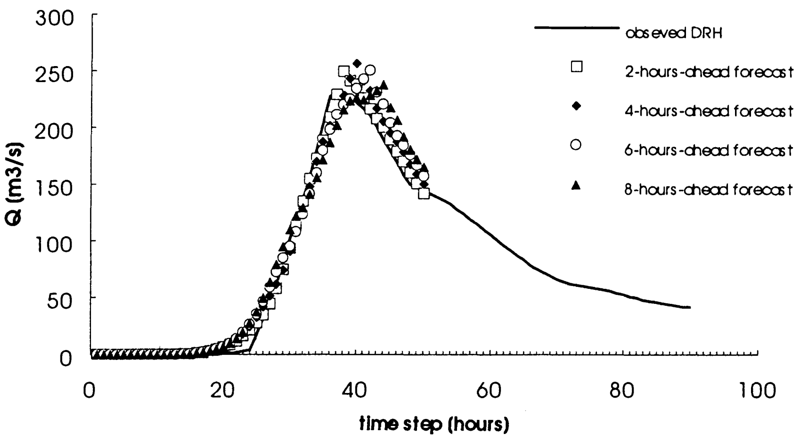

Fig. 7. Observed direct runoff hydrograph and 2-4-6-8 hours ahead forecasts by means of Extended Kalman Filter procedure for the May 1977 event. The value of σ was assumed to be 270 mm and initial condition C^*_0 to be 65 mm.

Conclusions

Three different approaches for updating a simple conceptual rainfall-runoff model and for its use for real time flood forecasting are investigated in this paper: the first two are based on an on-line parameter adjustment approach, the third one is based on the filtering of the state variables of the model through an Extended Kalman Filter formulation. The techniques are applied to the runoff production component of the model, which is defined by two parameters (σ, C^*_0). The first two techniques differ in the number of the parameters that are allowed to vary: in one case the two parameters are updated during the real time simulations, in the other case only the optimisation of the initial condition (C^*_0) is performed. It should be accounted for that the parameter updating procedure based on the on-line adjustment of the initial condition can be thought of as reinitializing of the model. The analysis is performed assuming a 'perfect foresight' scenario for the precipitation and is based on a lumped representation of the basin.

The comparison shows that the procedure based on the filtering techniques provides more reliable results in all but one the cases analysed, while the procedure based on the on-line calibration of both parameters badly trails behind the other two procedures. An explanation for these results is provided by the wide fluctuations of the parameter estimates carried out along the event, which seem to prevent a reliable use of the updated parameters during the forecast stage. As already suggested in the literature (see, for instance, Moore 1986), the lack of robustness characterises the parameter updating approach, since, at least in the cases investigated here, it merely serves to track the variations rather than to anticipate them. It is argued that the major source of forecasting error in the real time simulation exercise presented here is that due to the crude spatially lumped estimates of the precipitation input, based on few point measurements. So, the better performance obtained through the state updating procedure is not unexpected, because this procedures is particularly well-suited to compensate for the effect of past error-corrupted rainfalls on the internal states of the model which affects the identification of effective rainfall.

While we acknowledge the improvement obtained by applying the EKF, it should not be overlooked the vital role that the assumed dynamics and observation noises may play on the quality of the predictions (see, for instance, Puente and Bras 1987) and the difficulties arising in the identification of these error statistics. As suggested by these authors "depending on such noise parameters discharge predictions ... could range from unacceptable to excellent". In the light of these considerations, a parameter updating approach based on the on-line adjustment of the initial condition, such as the one presented here, could be regarded as a suitable option for adaptive forecasting with simple conceptual rainfall-runoff models. Other forms of state updating, based on an empirical approach which exploits the hydrologist's understanding of the physical mechanism operating, such as those proposed by Moore (1987), are under investigation.

References

Bacchi, B., Ranzi, R., and Borga, M. (1996) Statistical characterization of spatial patterns of rainfall cells in extratropical cyclones, *J. Geophys. Res., Vol. 101*, D21, pp. 26,277-26,286.

Bacchi, B., and Borga, M. (1993) Spatial correlation patterns and rainfall field analysis, *Excerpta, Vol. 7*, pp. 6-40.

Borga, M., and Vizzaccaro, A. (1996) On the interpolation of hydrologic variables: formal equivalence of multiquadratic surface fitting and kriging, *J. Hydrol.*, in press.

Borga, M., Capovilla, A., Cazorzi, F., and Fattorelli, S. (1991) Development and application of a real time flood forecasting system in the Veneto Region of Italy, *Wat. Resour. Manag., Vol. 5*, pp. 209-216.

Bras, R. L., and Rodriguez-Iturbe, I. (1985) *Random functions in hydrology*, Addison-Wesley Publ.

Brath, A., and Rosso, R. (1993) Adaptive calibration of a conceptual model for flash flood forecasting. *Wat. Resour. Res. , Vol. 29(8)*, pp. 2561-2572.

Chander, S., and Fattorelli, S. (1989) Adaptive gridsquare based geometrically distributed forecasting model. In: *Hydrological Applications of Weather Radar*, Cluckie, I. D. and Collier, C. G. (eds), Ellis Horwood, Chichester, UK, pp. 424-439.

Da Ros, D., and Borga, M. (1996) On the use of digital elevation model data for the derivation of the geomorphologic instantaneous unit hydrograph, *Hydrol. Processes*, in press.

Georgakakos, K. P. (1986) A generalized stochastic hydrometeorological model for flood and flash-flood forecasting, 1 – Formulation, *Wat. Resour. Res. , Vol. 22(13)*, pp. 2083-2095.

Georgakakos, K. P., and Smith, G. F. (1990) On improved hydrologic forecasting – results from a WMO real time forecasting experiments, *J. Hydrol., Vol. 114*, pp. 14-45.

Gupta, V. K., and Sorooshian, S. (1985) The automatic calibration of conceptual watershed models using derivative-based optimization algorithms, *Wat. Resour. Res., Vol. 21(4)*, 473-485.

Gupta, V. K., Waymire, E., and Rodriguez-Iturbe, I. (1986) On scales, gravity and network structure in basin runoff. In: *Scale Problems in Hydrology*, V. K. Gupta, I. Rodriguez-Iturbe and E. Wood (eds.). Dordrecht, Holland: D. Reidel, pp. 159-184.

Kirkby, M. J. (1976) Tests of random network model, and its application to basin hydrology, *Earth Surf. Proc., Vol. 1*, pp. 197-212.

Kitanidis, P. K., and Bras, R. L. (1980a) Real time forecasting with a conceptual hydrologic model. 1. Analysis of uncertainty, *Wat. Resour. Res. , Vol. 16(6)*, pp. 1025-1033.

Kitanidis, P. K., and Bras, R. L. (1980b) Real time forecasting with a conceptual hydrologic model. 2. Applications and results, *Wat. Resour. Res. , Vol. 16(6)*, pp. 1034-1044.

Mesa, O. J., and Mifflin, E. (1986) On the relative role of hillslope and network geometry in hydrologic response. In: *Scale Problems in Hydrology*, V. Gupta, I. Rodriguez-Iturbe and E. Wood (eds.). Dordrecht, Holland: D. Reidel, pp. 1-17.

Moore, R. J. (1985) The probability-distributed principle and runoff production at point and basin scales, *Hydrol. Sci. J., Vol. 30*, 2, pp. 273-297.

Moore, R. J. (1986) Advances in real time flood forecasting practice. Symposium on "Flood Warning Systems", Winter Meeting of the River Engineering Section, The Institution of Water Engineers and Scientist, UK, 23 pp.

Moore R. J. (1987) Towards more effective use of radar data for flood forecasting. In *Weather radar and Flood Forecasting*, V. K. Collinge and C. Kirkeby (eds), John Wiley and Sons Ltd., pp. 223-239.

Moore, R. J., and Clarke, R. T. (1981) A distribution function approach to rainfall-runoff modelling, *Wat. Resour. Res., Vol. 17(5)*, pp. 1367-1382.

Naden, P. (1992) Spatial variability in flood estimation for large catchments: the exploitation of channel network structure, *Hydrol. Sci, J., Vol. 37(1)*, pp. 53-71.

NERC (1975) *Flood Studies Report, Volumes I-V*, Natural Environment Research Council, London.

O'Connell, P. E., and Clarke, R. T. (1981) Adaptive hydrological forecasting – a review, *Hydrol. Sci. J., Vol. 26*, pp. 179-205.

Puente, C. E., and R. Bras, (1987) Application of nonlinear filtering in the real time forecasting of river flows, *Wat. Resour. Res., Vol. 23(4)*, pp. 675-682.

Serban, P., and Askew, A. J. (1991) Hydrological forecasting and updating procedures. In: *Hydrology for the water management of large river basin*, IAHS Publ. no. 201, pp. 357-369.

Sorooshian, S., and Dracup, J. A. (1980) Stochastic parameter estimation procedures for hydrologic rainfall-runoff models: correlated and heteroscedastic error cases, *Wat. Resour. Res., Vol. 16(2)*, pp. 430-442.

Todini, E. (1989) Flood forecasting models, *Excerpta, Vol. 4*, pp. 117-162.

Wood, E. F., and O'Connell P. E. (1985) Real time forecasting. In. *Hydrological Forecasting*, Anderson, M. G. and Burt, T. P. (eds.), Wiley and Sons Ltd., pp. 505-558.

WMO (1992) Simulated real time intercomparison of hydrological models, WMO Report no. 779, World Meteorol. Organization, Geneva, Switzerland.

Appendix A: On-line Parameter Estimation

The probability distribution function (*pdf*) used for describing the distribution of the storage capacity c in the PDM model is the Rayleigh function

$$f(c) = \frac{2c}{\sigma^2} \exp(-\frac{c^2}{\sigma^2}) \quad \text{(A1)}$$

$$F(c) = 1 - \exp(-\frac{c^2}{\sigma^2}) \quad \text{(A2)}$$

The relation between critical storage capacity C^* and storage volume S is expressed as

$$S(C^*) = \int_0^{C^*} \left(1-F(c)\right) dc = \sigma \frac{\sqrt{\pi}}{2} \operatorname{erf}(\frac{C^*}{\sigma}) \quad \text{(A3)}$$

where erf(z) represents the error function.

Optimisation Procedure and Parameter Estimation

The goal consists in the selection of a set of parameters that minimises the difference between the observed discharge and the computed discharge in terms of least squares errors. Thus, the objective function is defined as

$$Obj(\underline{\theta}) = \sum_{i=1}^{m} (Q_i^* - Q_i)^2 = \sum_{i=1}^{m} \varepsilon_i^2 = \underline{\varepsilon}^T \underline{\varepsilon} \quad \text{(A4)}$$

where Q^*_i and Q_i represents respectively the observed and the computed discharge value and m is the number of observations used for the calibration. In this specific case the n-dimensional vector of parameters is constituted by the two components

$$\underline{\theta}^T = [\theta_1 \; \theta_2]^T = [\sigma \; C_0^*]^T$$

Given the differentiability of the objective function the estimation of the parameters is achieved by the *Gauss-Newton's method.* It consists in the iterative computation of $Obj(\underline{\theta})$ in the maximum gradient direction of the space of parameters, defined by the condition

$$\underline{\theta}^{(s+1)} = \underline{\theta}^{(s)} + \alpha^{(s)} \underline{p}^{(s)} \quad \text{(A5)}$$

where $\alpha^{(s)}$ is a series of scalars that are selected in order to assure the convergence, and $\underline{p}^{(s)}$ is the vector that meets the condition

$$G(\underline{\theta}^{(s)}) \underline{p}^{(s)} = -\underline{g}(\underline{\theta}^{(s)}) = -2J(\underline{\theta}^{(s)})^T \underline{\varepsilon} \quad \text{(A6)}$$

and s denotes the iteration. The Hessian matrix G is defined as

$$G(\underline{\theta}) = 2\left(J(\underline{\theta})^T J(\underline{\theta}) + \sum_{i=1}^{m} \varepsilon_i G_i(\underline{\theta})\right) \quad \text{(A7)}$$

where the components of the Jacobian matrix (mxn) are computed as

$$J_{i,j} = \frac{\partial \varepsilon_i}{\partial \theta_j} = -\frac{\partial Q_i}{\partial \theta_j} \tag{A8}$$

while, from the component ε_i of the residuals vector, the elements of the Hessian matrix (nxn) are obtained through

$$(G_i(\underline{\theta}))_{j,h} = \frac{\partial^2 \varepsilon_i}{\partial \theta_j \partial \theta_h} = -\frac{\partial^2 Q_i}{\partial \theta_j \partial \theta_h} \tag{A9}$$

As suggested by Moore and Clarke (1981) the approximation $G(\underline{\theta}) \cong 2J(\underline{\theta})^T J(\underline{\theta})$ was adopted (*Gauss-Newton's method*). In this case the research equation simply reduces to

$$J^T(\underline{\theta}^{(s)})J(\underline{\theta}^{(s)})\underline{p}^{(s)} = -J^T(\underline{\theta}^{(s)})\underline{\varepsilon} \tag{A10}$$

Computation of the Jacobian Matrix components:

The runoff produced at time $k\Delta t$ is computed from

$$V_k = (C_k^* - C_{k-1}^*) - \sigma\frac{\sqrt{\pi}}{2}\left(\mathrm{erf}\left(\frac{C_k^*}{\sigma}\right) - \mathrm{erf}\left(\frac{C_{k-1}^*}{\sigma}\right)\right) \tag{A11}$$

Hence, in this problem Eq. (A.8) becomes

$$J_{i,j} = \frac{\partial \varepsilon_j}{\partial \theta_j} = -\frac{\partial Q_j}{\partial \theta_j} = -\frac{\partial}{\partial \theta_j}\left(\sum_{k=1}^{i} V_k u_{i-k+1}\right) = -\sum_{k=1}^{i} u_{i-k+1}\frac{\partial V_k}{\partial \theta_j} \tag{A12}$$

Taking into account that $C^*_k = C^*_0 + \sum_{i=1}^{k} \pi_i$ and $C^*_{k-1} = C^*_0 + \sum_{i=1}^{k-1} \pi_i$, where $\pi_i = p_i \Delta t$ denotes the rainfall aggregated in the interval Δt, the computation of the derivatives of $\underline{V}$ results

$$\frac{\partial V_k}{\partial \theta_1} = \frac{\partial V_k}{\partial \sigma} = \frac{1}{\sigma}\left(C_k^* \exp\left(-\frac{C_k^{*2}}{\sigma^2}\right) - C_{k-1}^* \exp\left(-\frac{C_{k-1}^{*2}}{\sigma^2}\right)\right) + - \frac{\sqrt{\pi}}{2}\left(\mathrm{erf}\left(\frac{C_k^*}{\sigma}\right) - \mathrm{erf}\left(\frac{C_{k-1}^*}{\sigma}\right)\right) \tag{A13}$$

$$\frac{\partial V_k}{\partial \theta_2} = \frac{\partial V_k}{\partial C_0^*} = -\exp\left(-\frac{C_k^{*2}}{\sigma^2}\right) + \exp\left(-\frac{C_{k-1}^{*2}}{\sigma^2}\right) \tag{A14}$$

Appendix B: Application of the Extended Kalman Filter

The system under consideration at time t may be described by the following equations

$$\underline{X}_t = \Phi \underline{X}_{t-1} + \underline{G}\underline{U}_t + \underline{\Gamma} w_t \qquad \text{state equation} \tag{B1}$$

$$z_t = h(\underline{X}_t) + v_t \qquad \text{observation equation} \tag{B2}$$

with w_t and v_t being the independent discrete dynamics and observations Gaussian white-noises with variances Q_t and R_t respectively. The vector X_t $((n+1)\times 1)$ represents the state variable

$$\underline{X}_t = \begin{bmatrix} X_1^t \\ X_2^t \\ \dots \\ X_{n-1}^t \end{bmatrix} = \begin{bmatrix} C_t^* \\ C_{t-1}^* \\ \dots \\ C_{t-n}^* \end{bmatrix} \quad (n+1)\times 1 \text{ with } C_{t-j}^* = C^* \text{ if } \quad t-j \leq 0 \tag{B3}$$

where n is the dimension of the vector corresponding to the Unit Hydrograph. Let $P_{t|t}$ denote the state estimate error covariance matrix $P_{t|t}$ at time t obtained from information up to time t, with initial conditions

$$\underline{X}_0 = \begin{bmatrix} C_0^* \\ C_0^* \\ \dots \\ C_0^* \end{bmatrix} \qquad P_0 = \sigma_{C_0^*}^2 \begin{bmatrix} 1 & 1 & \dots & 1 \\ 1 & 1 & \dots & 1 \\ \dots & \dots & \dots & 1 \\ 1 & 1 & 1 & 1 \end{bmatrix}$$

The matrix Φ is as follows

$$\Phi = \begin{bmatrix} 1 & 0 & 0 & 0 & \dots & 0 \\ 1 & 0 & 0 & 0 & \dots & 0 \\ 0 & 1 & 0 & 0 & \dots & 0 \\ 0 & 0 & 1 & 0 & \dots & 0 \\ \dots & \dots & \dots & \dots & \dots & 0 \\ 0 & 0 & 0 & 0 & 1 & 0 \end{bmatrix}$$

and $U_t = \pi_t$ denotes the rainfall aggregated in the interval $(t\text{-}\Delta t,\ t)$ and represents the input variable.

$$\underline{G}^T = \underline{\Gamma}^T = \begin{pmatrix} 1 & 0 & \dots & 0 \end{pmatrix}^T \qquad 1\times(n+1)$$

The discharge at the basin outlet is the observation variable; the observation equation is a scalar one and can be expressed as

$$h(\underline{X}_t) = \underline{u}^T \underline{V}_t = \sum_{i=1}^{n} u_i V_i^t = \sum_{i=1}^{n} u_i \int_{C_{t-i}^*}^{C_{t-i+1}^*} F(c)\,dc = \sum_{i=1}^{n} u_i \int_{X_{i+1}^t}^{X_i^t} F(c)\,dc \tag{B4}$$

Its linearization is obtained through the first order derivatives with respect to the state variable

$$h(\underline{X}_t) \cong h(\hat{\underline{X}}_{t|t-1}) + \left.\frac{\partial h(\underline{X}_t)}{\partial \underline{X}_t}\right|_{\underline{X}_t=\hat{\underline{X}}_{t|t-1}} (\underline{X}_t-\hat{\underline{X}}_{t|t-1}) = h(\hat{\underline{X}}_{t|t-1}) + H_t(\underline{X}_t-\hat{\underline{X}}_{t|t-1}) \tag{B5}$$

where

$$H_t = [u_1, u_2, \ldots, u_n] \begin{bmatrix} F(X_1^t) & -F(X_2^t) & 0 & \ldots & 0 \\ 0 & F(X_2^t) & -F(X_3^t) & \ldots & 0 \\ 0 & 0 & F(X_3^t) & \ldots & 0 \\ \ldots & \ldots & \ldots & \ldots & 0 \\ 0 & 0 & 0 & F(X_n^t) & -F(X_{n+1}^t) \end{bmatrix}_{\underline{X}_t=\hat{\underline{X}}_{t|t-1}} \tag{B6}$$

The Extended Kalman filter algorithm is then expressed as

Forecast (at time t):

$$\hat{\underline{X}}_{t+1|t} = \Phi\hat{\underline{X}}_{t|t} + \underline{G}U_{t+1}$$

$$P_{t+1|t} = \Phi P_{t|t}\Phi^T + \underline{\Gamma}Q_t\underline{\Gamma}^T$$

At any observation (at time t+1):

$$K_{t+1} = P_{t+1|t}H_{t+1}^T(H_{t+1}P_{t+1|t}H_t^T + R_{t+1})^{-1}$$

$$\hat{\underline{X}}_{t+1|t+1} = \hat{\underline{X}}_{t+1|t} + K_{t+1}\left(z_{t+1} - h(\hat{\underline{X}}_{t+1|t})\right)$$

$$P_{t+1|t+1} = (I - K_{t+1}H_{t+1})P_{t+1|t}(I - K_{t+1}H_{t+1})^T + K_{t+1}R_{t+1}K_{t+1}^T$$

Received: 20 January, 1997
Revised: 18 June, 1997
Accepted: 30 June, 1997

Address:
Department of Land and Agroforest Environments,
AGRIPOLIS, University of Padova,
via Romea, 35020 Legnaro, Padova,
Italy.